

# Space structure with developable shear components

## *Estructura espacial con elementos a cortante desarrollables*

Nicolas Leduc<sup>a, c</sup>, Cyril Douthe<sup>a</sup>, Gérald Hivin<sup>b</sup>, Bernard Vaudeville<sup>c</sup>, Simon Aubry<sup>c</sup>,  
Karine Leempoels<sup>d</sup>, Olivier Baverel<sup>a, e</sup>

<sup>a</sup> Laboratoire NAVIER, Ecole des Ponts ParisTech, 6 - 8 Avenue Blaise Pascal, Champs sur Marne, 77455 Marne la Vallée Cedex 2, France

<sup>b</sup> Université Grenoble-Alpes, 621 Avenue Centrale, 38400 Saint-Martin-d'Hères, France

<sup>c</sup> T/E/S/S Atelier d'Ingénierie, 7 Cité Paradis, 75010 Paris, France

<sup>d</sup> Viry, 5, ZI de la Plaine - Eloyes, 88214 Remiremont Cedex, FRANCE

<sup>e</sup> École Nationale Supérieure d'Architecture de Grenoble, 60 Avenue de Constantine, 38000 Grenoble, France

Recibido el 25 de diciembre de 2019; aceptado el 2 de septiembre de 2020

This paper has been presented at the International fib Symposium on Conceptual Design of Structures held in Madrid in September 2019

### ABSTRACT

The classical double layer space truss is revisited by replacing diagonals with curved thin-walled polyhedral modules. The expected improvements are both technological and mechanical. The complex 8-branch nodes are broken down into a connection of two overlapping continuous members and a line connection between bars and the polyhedron edges. Curvature in the faces and edges of the modules introduces shape resistance whilst stabilizing the members against buckling. The global optimization of the structure is performed by a form-finding process based on the individual parametrization of the modules. Finally, an experimental validation is carried out by fabricating and testing a full-scale prototype (approximately 6 x 6 m).

© 2021 Asociación Española de Ingeniería Estructural (ACHE). Published by Cinter Divulgación Técnica S.L. All rights reserved.

KEYWORDS: Form finding; space structure; parametric design; steel; detailing; construction aware design.

### RESUMEN

En este artículo se revisita la clásica cercha espacial de doble pared reemplazando las diagonales por módulos poliédricos curvos de paredes delgadas. Las mejoras esperadas son tanto tecnológicas como mecánicas. Los nodos complejos de 8 ramas se dividen en una conexión de dos miembros continuos superpuestos y una conexión lineal entre las barras y los bordes del poliedro. La curvatura en las caras y bordes de los módulos introduce resistencia por forma y estabiliza los miembros frente al pandeo. La optimización global de la estructura se realiza mediante un proceso de búsqueda de forma basado en la parametrización individual de los módulos. Finalmente, se lleva a cabo una validación experimental mediante la fabricación y prueba de un prototipo a escala real (de 6 x 6 m aproximadamente).

© 2021 Asociación Española de Ingeniería Estructural (ACHE). Publicado por Cinter Divulgación Técnica S.L. Todos los derechos reservados.

PALABRAS CLAVE: Búsqueda de forma; estructura espacial; diseño paramétrico; acero; diseño consciente de la construcción.

## 1. INTRODUCTION

The classification of spatial structures generally falls into three broad categories [1]: skeleton (braced) framework, stressed skin systems and suspended (cable or membrane) structures.

We describe here the process of designing and manufacturing a structure that combines the first two. From the first category it inherits an upper and lower layer consisting of a two-way lattice grid. From the second category it inherits shear components made up of curved thin-walled polyhedral modules.

\* Persona de contacto / Corresponding author.  
Correo-e / email: [nico.leduc@gmail.com](mailto:nico.leduc@gmail.com) (Nicolas Leduc).

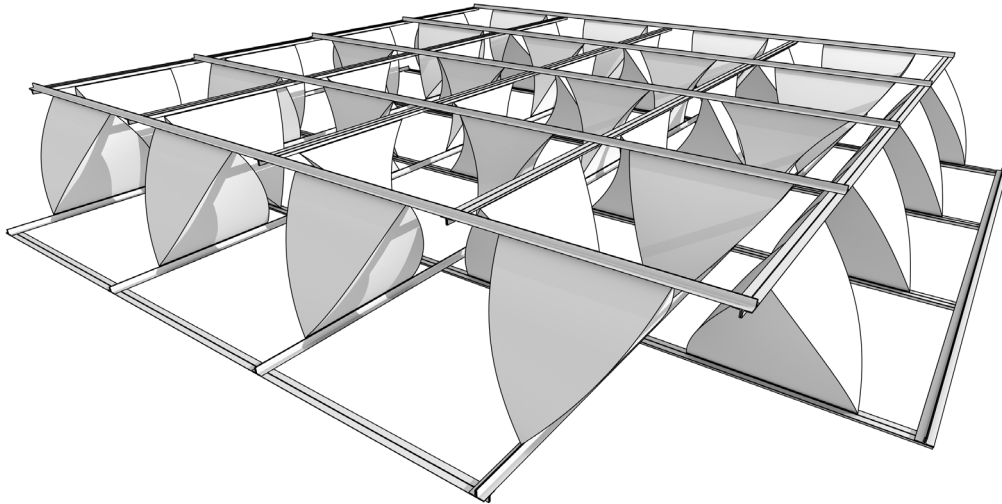


Figure 1. Perspective view of the prototype.

As identified in [2], the greatest set-back against the increased use of space structures is the technological complexity of assembling several members at different angles in space. After Wachmann's attempt to design a universal node [3], more specific ones were developed for patented systems or in the context of particular projects [4].

The strategy we are developing here is to break down this complexity into two simple connections: a connection of two overlapping continuous members (upper and lower layer) and a line connection between bars and the polyhedron edges. A similar approach has already been tested in [5]. Beyond the technological advantages, the issue of mechanical performance is also addressed: the question of instabilities is a critical subject in the case of slender bars and thin sheet metals. Curvature in the faces and edges of the modules introduces shape resistance while stabilizing the members against buckling.

This approach is implemented as a full-scale prototype whose design steps are used to structure the article as follows. Section 2 presents the layout of the modular grid resulting from the semi-regular tessellation of space. Section 3 focuses on a single module by describing its structural behaviour and geometric parameterisation that provide the basis for the form-finding optimisation that is described in section 4. Finally, section 5 deals with manufacturing issues.

## 2. SPATIAL LAYOUT OF THE MODULAR GRID

Double-layer space structures are generally modular, i.e. they have a spatial periodicity. It is common to base the design of such structures on regular tessellation of the space, as the famous engineer Alexander Graham Bell did for the development of his flying machines [6]. The vertices of the polyhedra then correspond to the nodes of the structure and the edges correspond to the bars.

There are different types of periodic tessellation of space (regular, semi-regular, etc.), only some of which have the necessary stability properties for use as a structure. The prototype developed here is based on the only semi-regular tessellation, consisting of a concatenation of tetrahedrons and octahedrons.

Unlike Alexander Graham Bell who, in his experiments on kites, expanded the structure in three directions of space, the double-layer space structure is a two-dimensional truncation of the polyhedra concatenation. This operation keeps a layer of tetrahedrons and transforms the octahedrons into square-based pyramids with apex oriented alternately upwards or downwards.

In accordance with the classical approach, the vertices and edges of the upper and lower faces are associated with

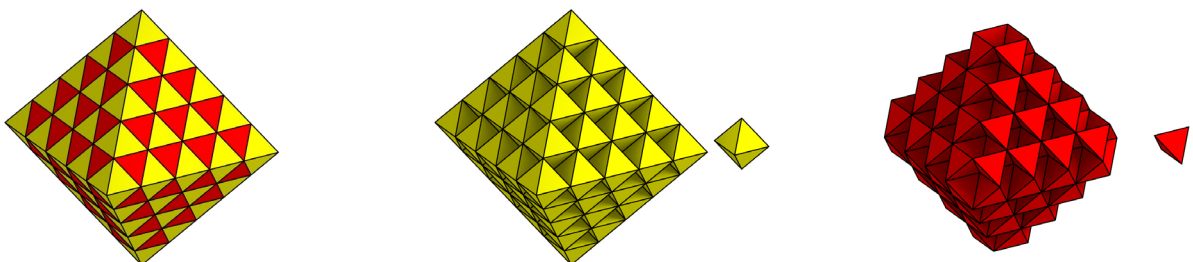


Figure 2. Semi-regular tessellation composed of alternating regular octahedra and tetrahedra.

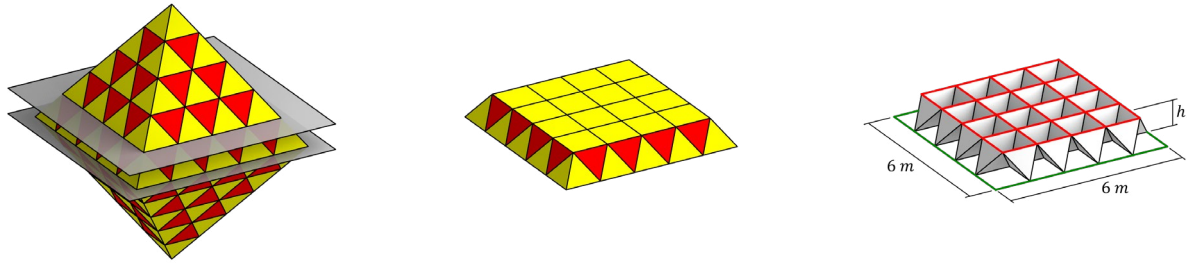


Figure 3. Left and Middle: The space-filling polyhedra are sliced off by a truncation operation, Right: Spatial layout of the modular grid and its main dimensions.

the nodes and horizontal members of the structure. However, the surface geometry of the tetrahedral modules is preserved to play the role of diagonals. Square-based pyramids can be read in negative.

For the prototype presented here, the maximum dimensions are 6x6 m, i.e. a lower grid composed of 5 cells of 1.2m in both directions. The upper grid, being offset by half a frame in both directions, is composed of only 4 cells. The vertical distance between the two layers is noted  $h$  and is not fixed a priori. It will be part of the variables for the global optimization of the structure explained below.

### 3. STUDIES AT THE MODULE SCALE

#### 3.1. Geometric parameterization

In addition to the layout of the modular grid, four parameters specify the geometry of the module considering its double symmetry (according to the YZ and ZX planes).

The first parameter ( $0 < \mu < 1$ ) only affects the position of the vertices of the tetrahedron along the members on which it is connected. If  $\mu = 1$ , the structure adopts a triangulated lattice configuration while if  $\mu < 1$ , the structure adopts a Vierendeel configuration.

The other three parameters ( $\theta, \varphi, r$ ) affect the geometry of the faces defined as general cylinders whose edges are three-dimensional curves (cubic Bézier curve). More precisely, these three parameters define the curve by its tangents at the ends in a local polar coordinate system. In this way,  $(\theta, \varphi)$  define the direction and  $r$  the norm of the vector.

Given the overall definition of the grid and the symmetry conditions on the module, these four parameters are sufficient to uniquely define the geometry of the curved tetrahedron.

#### 3.2. Structural behaviour

In a double-layer space structure under bending loading, the lower and upper horizontal members carry predominantly tension and compression. The intermediate elements, in this case the tetrahedral modules, support the shear stresses. To better understand the subsequent global optimization, we show the results of a first study of a single module under a typical shear load case.

We compare the displacement ( $\delta$ ) and buckling load factor ( $LF$ ) values for a fixed position of the vertices ( $\mu = 0.6$  and  $h = 0.6$  m) and constant amount of material for two case studies made of steel S235. The first case is optimized to minimize displacement and happens to be the flat thin-walled polyhedral module (FM). It is chosen as the reference module with a 1.5 mm thick steel sheet. The second case is opti-

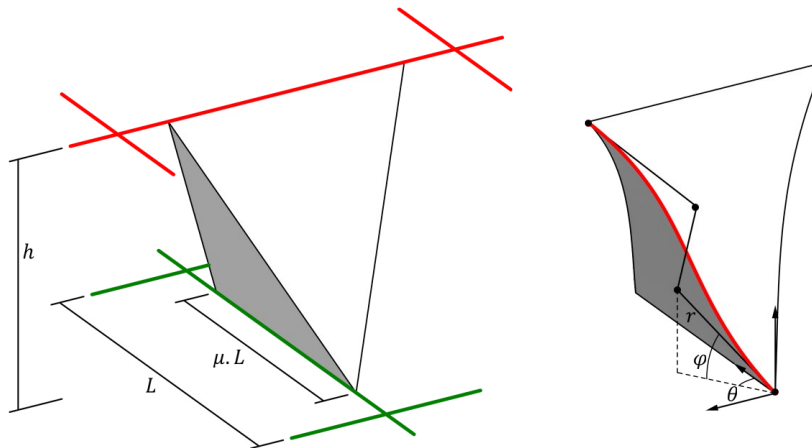


Figure 4. Four parameters ( $\mu, \theta, \varphi, r$ ) define the local geometry of a tetrahedron (in addition to  $h$  and  $L$ ). As defined above,  $L = 1.2$  m in the built prototype.

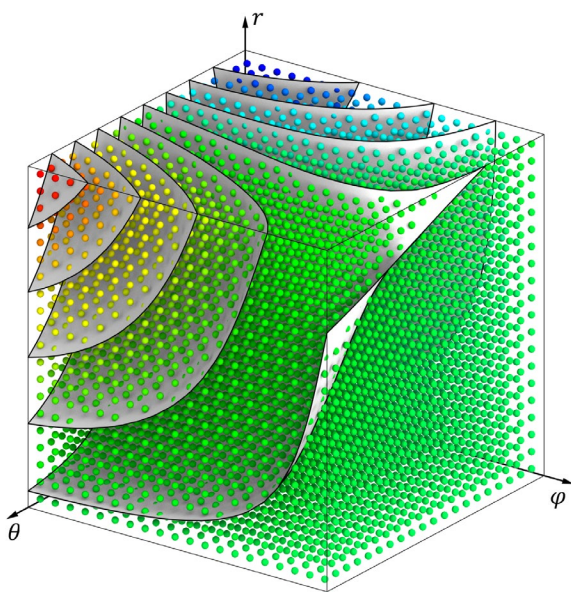
mized to maximize buckling load factor. The thickness of this curved thin-walled polyhedral module (CM) is set so that the weight is the same as the flat module. For information only, a third module made of bars (BM) is added to the list. The latter could not compete without considering more broadly the technological difficulty of its connections. The bars are Circular Hollow Sections (CHS) with wall thickness 3mm. The external diameter is set so that the weight is the same as the flat module.

TABLE 1.  
Table comparing three case studies for the following results: displacement ( $\delta$ ) and buckling load factor (LF)

Case	$\delta$ (absolute)	$\delta$ (relative)	LF (absolute)	LF (relative)
FM	0.12 mm	100%	1.3	100%
CM	0.73 mm	608%	11.6	892%
BM	0.16 mm	133%	39.7	3053%

It must be noted that the flat module has better shear stiffness due to a more efficient transmission of forces through a straight fold. However, when the morphology of the module has been optimized to maximize buckling resistance, the curvature introduced into the faces improves buckling resistance by a factor of 9, an essential feature when working with thin sheet metal.

The second study consists of looking at the solution space of a module with curved faces by varying the parameters ( $\theta, \varphi, r$ ). As in the previous study, the results of displacement and buckling load factor are calculated for a given vertex position and amount of material. The sheet metal area is also measured. Each set of parameters ( $\theta, \varphi, r$ ) can be represented by a point in a three-dimensional Cartesian space and is associated with a displacement, buckling load factor and area value as shown in Fig 5 (left).



It is noteworthy that iso-value surfaces reveal the non-convexity of the three observed functions (displacement, buckling load factor and area). This will guide our choice in the type of algorithm to be implemented for optimizations.

Beyond the representation of the solution space of a single function, crossing maps of the kind shown in figure 5 (left), is an effective way to visualize which modules meet several requirements simultaneously as illustrated in figure 5 (right).

## 4. STUDIES AT THE FULL PROTOTYPE SCALE

### 4.1. Optimisation settings

Previous studies have shown that the modules have very different structural properties depending on their morphology. Conversely, depending on the location of the module within the prototype, the forces applied vary and the parametric tetrahedron can adapt its shape to improve its structural behaviour. Essentially, except for the extra effort at the design stage, the generation of different modules has little impact on the manufacturing process since the thin steel sheet faces of the tetrahedrons are laser cut and the elastic shaping process avoids the need for formwork and bending machines.

Hence, to determine the shape of each tetrahedron, we decided to conduct a form finding step at first. The structure is subjected to a vertical load of 1.5 kN applied to each node of the lower grid (total load: 24 kN) and is supported on the 16 peripheral nodes. The double symmetry of geometry, loading and supports is considered to determine the number of distinct modules (6) and to simplify the calculation models. The geometry of each module being defined by 4 parameters ( $\mu, \theta, \varphi, r$ ) and considering the structural height parameter ( $h$ ) defined above, the prototype model is completely determined by 25 parameters.

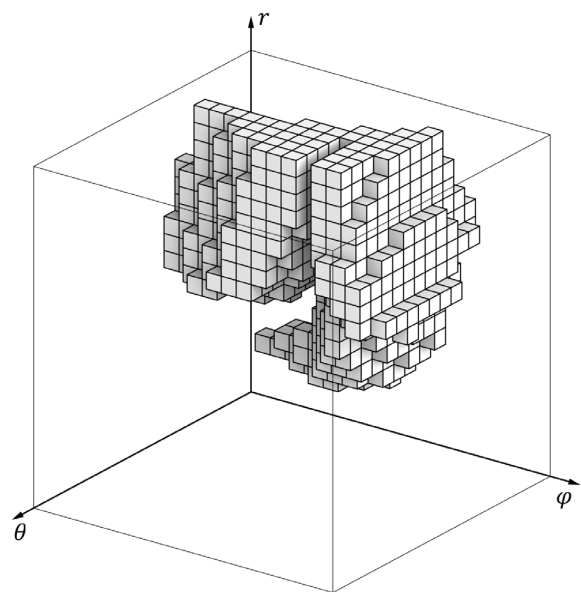


Figure 5. Left: Color code representing the area value in the three-dimensional space ( $\theta, \varphi, r$ ). Iso-value surfaces are plotted in the same space. Right: 3D Map of the modules which satisfy the triple constraint  $\delta < 10\text{mm}$ ,  $LF > 5$  and  $0.75 < A < 1.00 \text{ m}^2$ .



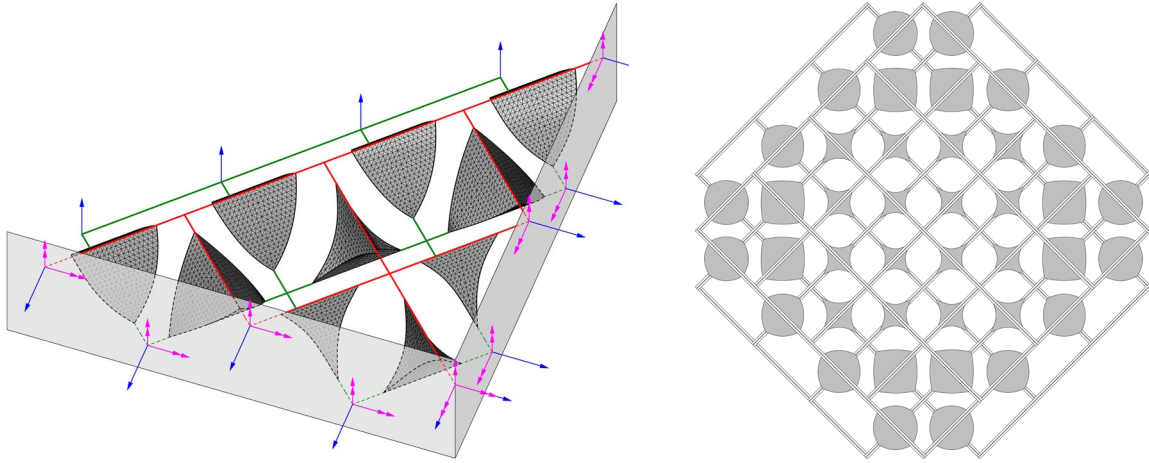


Figure 6. Support condition applied on a quarter of the model (single blue arrow: Translational support, double magenta arrow: Rotational support). Right: Plan view showing the distribution of the optimized modules.

A constrained optimization is carried out with the dual objective of improving mechanical behaviour (maximization of the buckling load factor) and reducing the quantity of material (minimization of the area of the tetrahedrons). The following hard constraints are additionally prescribed:

- maximum deflection must be less than 30 mm (two hundredths of the span)
- bending radius of the sheets must be greater than 1m in order to remain in the elastic range.

Given the non-convexity of the buckling load factor and area functions to be processed, a global optimization algorithm (DIRECT algorithm [7]) is coupled with a structural analysis software (Karamba3d) in the graphical algorithm editor Grasshopper integrated with Rhino's 3-D modeling tools.

#### 4.2. Results

The results of the optimization qualitatively follow the shear stress distribution (maximum at the edges) of a continuous plate with similar loading and support conditions.

For a quantitative interpretation, we compare the optimized result (Curved Modules CM) with a flat tetrahedral solution (Flat Modules FM) of the same structural height and same parameter  $\mu$  as the optimized solution.

Taken as a whole, the solution with Curved Modules (CM) has a clear advantage over that with Flat Modules (FM). With comparable values of deflection and amount of material, the curved module structure has a buckling factor four times higher.

TABLE 2.

Table comparing two case studies for the following results: maximum displacement ( $\delta$ ), buckling load factor ( $LF$ ), area ( $A$ ) and total weight of the structure ( $W$ )

Case	$\delta$ (abs)	$\delta$ (rel)	$LF$ (abs)	$LF$ (rel)	$A$ (abs)	$A$ (rel)	$W$ (abs)	$W$ (rel)
CM	3.77mm	100%	13.17	100%	40.1m <sup>2</sup>	100%	805kg	100%
FM	3.56mm	94%	3.6	27%	39.1 m <sup>2</sup>	98%	766kg	95%

## 5.

### FABRICATION

What better proof of concept regarding technological simplicity than having the prototype assembled by non-professionals? The prototype was built in an academic context by four students. At the rate of half an hour per module, the structure was assembled in 4 days.

#### 5.1. Building materials

The four panels of each module are made of galvanised carbon steel, grade S235. Their average dimensions (enclosed in a square of 0.8m size) and thickness directed the choice towards laser cutting. Each member of the upper and lower grids consists of a double L profile (30.30.3) made of galvanised carbon steel S235. All assemblies are carried out by a single type of bolt but with three lengths of shank: Button Head Screw BHS M6 (shank length 10/12/14mm) and cap nut.

#### 5.2. Assembly

The assembly steps were as follows:

- Sorting of the different components of the modules which came in a random sequence due to the nesting optimisation for the laser cutting: Figure 7 (Left)
- Prefabrication and storage of the 40 modules: Figure 7 (Middle Left)
- Pre-assembly of the lower grid on the ground
- Assembly of the modules on the lower grid: Figure 7 (Middle Right)
- Assembly of the upper grid on the modules: Figure 7 (Right)
- Lifting by overhead crane onto the supports: Figure 10

#### 5.3. Assembly detail

The upper and lower grids are made of overlapping continuous members connected by four button head screws at each

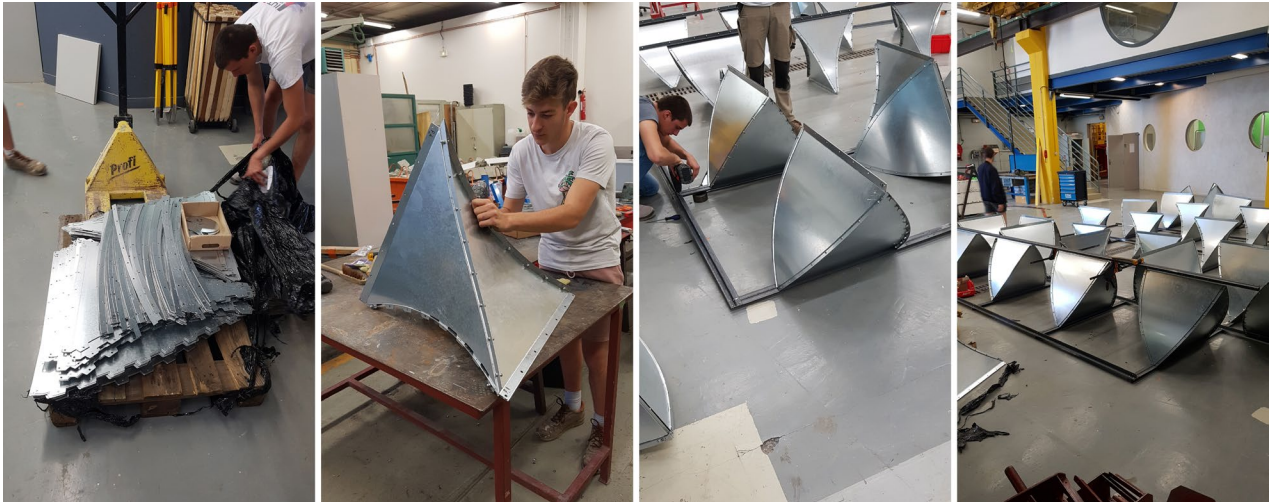


Figure 7. Assembly steps of the prototype. Left: One pallet is sufficient to hold all the sheet metals of the modules. Middle left: Pre-assembly of a concave module. Middle right: Assembly of the modules on the lower grid is carried out on the ground. Right: Assembly of the upper grid on the modules.

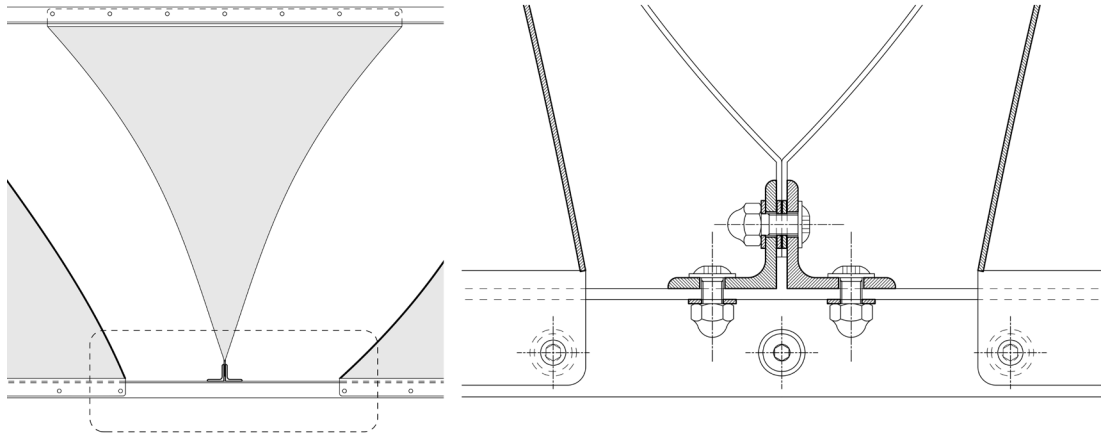


Figure 8. Cross section on connection detail between tetrahedrons and lower grid.

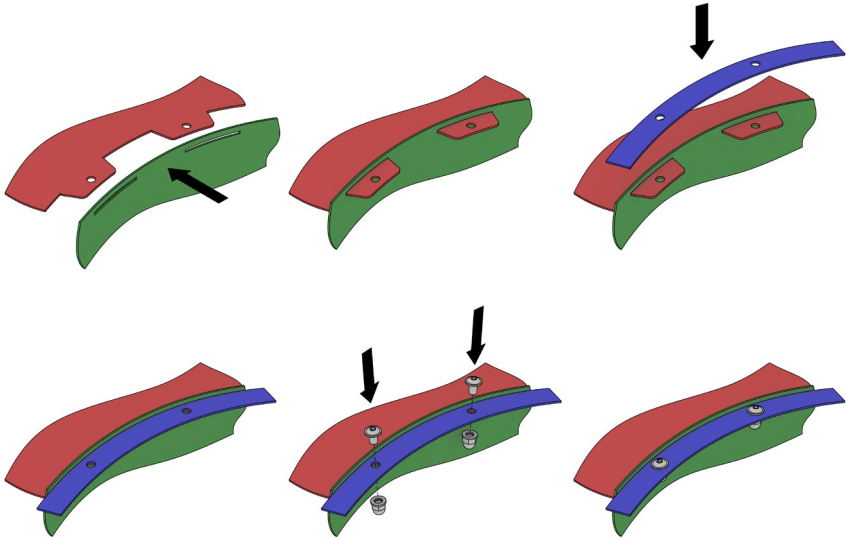


Figure 9. Assembly kinematics of the curved edge.



Figure 10. Prototype assembled in the testing centre of the Université Grenoble-Alpes, civil engineering department.

intersection. The modules are fastened to the members by a narrow folded strip that is pinched between the two L profiles.

The principle of assembly of the curved edge is closed to a keyed mortise and tenon joint. Panel 1 (in red) with a tenon is inserted inside the mortise of Panel 2 (in green). A curved and narrow strip (in blue) overlaps the tenon and prevents the connection from loosening. At the end, the assembly is locked by the key (button head screw, cap nut and washers).

## 6. CONCLUSIONS AND DISCUSSIONS

We have shown, through the construction-aware design of the prototype, the advantages of this hybrid spatial structure: with a simplified technological implementation and high structural performances resulting from the form-finding process. The result is a strong architectural expressiveness of the forces that pass through the structure.

Metrological studies based on image correlation are currently being carried out. They will allow us to experimentally describe the structural behaviour of the prototype and give us feedback on numerical simulations.

The complexity of this prototype has been deliberately limited due to time and resources. It would be useful to understand what advantages could be achieved by studying other spatial tessellations instead of the classical tetrahedron/octahedron layout or by applying this structural typology not only to slabs but to shell geometries.

## Acknowledgements

We thank Guillaume Galpin, Gabriel Thivillier, Vincent Loisy and Eugène Hortefeux, students at Université Grenoble-Alpes, civil engineering department, who assembled and tested the prototype as part of their final year study project

## References

- [1] Makowski, Z.S. (1965). *Steel Space Structures*. London: Michael Joseph.
- [2] Subramanian, N. (1999). *Principles of space structures*. New Delhi: Wheeler.
- [3] Makowski, Z.S. (2002). Development of jointing systems for modular prefabricated steel space structures. Paper presented at the meeting Lightweight Structures In Civil Engineering. Warsaw, Poland, June 24–28
- [4] Stephan, S., Sánchez-Álvarez, J. & Knebel, K. (2004). Reticulated structures on free-form surfaces. *Stahlbau* 73(8), 562–72.
- [5] Baverel, O., Chalas, P., Richefeu, V. & Hivin, G. (2018). Proposal for a low tech wooden space truss. Paper presented at the annual meeting for International Association of Space Structures, Boston, United States, July 16–20.
- [6] Bell, A.G. (1903). Tetrahedral principle in kite structures. *National Geographic Magazine* 14(6), 219–251.
- [7] Jones, D.R., Perttunen, C.D. & Stuckman, B.E. (1993). Lipschitzian optimization without the Lipschitz constant. *Journal of optimization Theory and Applications*, 79(1), 157–181.